Multichannel reflectance spectral assaying of zinc and copper flotation slurries

Olli Haavisto *, Jani Kaartinen

Helsinki University of Technology (TKK), Department of Automation and Systems Technology, P.O. Box 5500, FI-02015 TKK, Finland

ABSTRACT

This article extends the earlier work (Haavisto et al. 2008. Optical spectrum based measurement of flotation slurry contents. Int. J. Miner. Process. 88 (3–4), 80–88), where visible and near-infrared (VNIR) reflectance spectroscopy was used together with an X-ray fluorescence (XRF) analyzer to improve the assaying of zinc flotation concentrate. Especially the sampling interval of the assay could be drastically reduced by the presented approach. In this study, a multichannel VNIR spectrum analyzer is utilized to measure the spectrum of the seven most important slurry lines in copper and zinc flotation circuits. Recursive data-based modeling is applied to the VNIR spectrum data and XRF assays to calculate and adaptively maintain the calibration model. The accuracy of the VNIR assays is evaluated in all the lines, and the benefits of the obtained high frequency assays in detecting oscillations and sudden grade changes are demonstrated.

© 2009 Elsevier B.V. All rights reserved.

1. Introduction

Monitoring and control of mineral flotation processes is mainly based on the on-line assaying of the slurry flows. The most common automatic assaying technique is X-ray fluorescence (XRF) analysis, where slurry is radiated with X-rays and the spectrum of the reflected fluorescent radiation is used to determine the elemental contents of the slurry. At larger flotation plants sample lines from the main slurry flows are led to one or more centralized on-line XRF analyzers.

Compared to manual laboratory analysis the introduction of the XRF analyzers in the 1970s released the plant personnel from the laborious analysis work and provided the means for automatic process monitoring and control (McKee, 1991). However, as pointed out, for example, by Bartolacci et al. (2006) and Liu and MacGregor (2008), the drawback of a centralized XRF analyzer is the sparse sampling interval for a single slurry line. Several slurry lines are measured by the same analyzer in turns, and in a typical setup the time between two consecutive assays from one slurry line can be around 10–20 min. Therefore in some cases the most critical slurry lines have to be sampled twice during the analyzer cycle, which further increases the delay in the other lines.

The earlier phase (Haavisto et al., 2008) of this work introduced the visible and near-infrared (VNIR, 400–1000 nm) reflectance spectroscopy as a tool for improving the sparse XRF assays of zinc concentrate slurry. Originally, the reflectance spectroscopic analysis of minerals has mostly been conducted in the field of remote sensing, where it has been utilized, for example, to study the composition of planet surfaces or to create mineralogical maps using imaging spectroscopy data gathered from satellites or aircraft (Clark, 1999). In mineral processing,

reflectance spectroscopy can also be used to analyze the mineral composition of drill cores as a lightweight option for laser-induced breakdown spectroscopy (LIBS) or X-ray diffraction (XRD) (Kruse, 1996). On the other hand, the color information acquired by regular red–green–blue (RGB) cameras has been used as an important variable in many froth classification and grade estimation studies (Bartolacci et al., 2006; Morar et al., 2005; Liu et al., 2005; Kaartinen et al., 2006). Haavisto et al. (2006) further compared the RGB data and VNIR reflectance spectroscopy in froth grade estimation.

In this study, the initial slurry VNIR spectrum analysis reported by Haavisto et al., (2008) is extended to cover seven different slurry lines at a copper and zinc flotation plant. First, the structure and properties of the flotation process and the analyzed slurry lines are detailed and the measurement setup is presented. Then, the data collection and modeling are explained and the obtained results are reported and discussed.

2. Materials and methods

The measurements and analysis for this study were conducted at the Inmet Mining Corporation's Pyhäsalmi zinc, copper and sulfur mine located in central Finland. The concentration at Pyhäsalmi is performed sequentially in three stages: copper is first floated from the milling product in the copper flotation circuit, zinc is then separated from the copper tailings in the zinc circuit, and, finally, the zinc tailings are processed in the sulfur circuit to float the sulfur. Copper and zinc are the most important products of the plant, and thus the focus of this study is on the copper and zinc circuit slurries. These circuits both consist of rougher, scavenger, middlings flotation and cleaner stages and are monitored by the same centralized on-line XRF analyzer (Outotec Courier® 6 SL). For each slurry flow, the iron, copper

and zinc elemental contents are directly measured by the analyzer, and sulfur content is calculated from these. Additionally, the solids content measurement is provided by the analyzer.

2.1. Materials

The main minerals in the slurry flows of the analyzed concentration plant are pyrite (FeS_2), sphalerite ($Zn_XFe_{1-X}S$, where $X \approx 0.95$), chalcopyrite ($CuFeS_2$) and pyrrhotite ($Fe_{1-Y}S$, where Y varies from 0 to 0.17). Also minor amounts of galena (PbS) and sulfosalts are present. The main gangue minerals are barite ($BaSO_4$) and carbonates. The particle size of the flotation circuit feed after milling is about 65% −74 µm.

The optical properties of the main minerals can be analyzed by comparing the reflectance spectra measured under laboratory conditions. Fig. 1 shows the hemispherical reflectance spectra (see e.g. Hapke, 1993) of the three most important minerals in two particle size classes measured from dry mineral samples. The data were gathered from the ASTER spectral library (http://speclib.jpl.nasa.gov/).

2.2. Measurement setup

The measurement principle of the multichannel slurry spectrum analyzer, as shown in Fig. 2, is similar to the one presented by Haavisto et al., (2008). However, in this case the analysis equipment is packed into a specially designed enclosure that is relatively small in size and lightweight. This makes it possible to conveniently install several of these analyzer boxes right before the secondary sampler of the XRF analyzer (see Fig. 3). The spectrograph is essentially the same Specim ImSpector V10 combined with the Basler A102f camera as in Haavisto et al. (2008), the only difference being that the imaging optics is replaced with a bundle of 7 optical fibers. The common end of the bundle is attached in front of the entrance slit of the spectrograph so that the fibers are positioned next to each other. The other ends of the fibers are directed to the analyzer boxes and equipped with collimator lenses that capture the light reflected from a round area (diameter 11 mm) in the middle of the jet flow cell window. Illumination of the slurry in each line is accomplished by a halogen lamp (12 V, 10 W, 3000 K) that is equipped with an axial silver coated

reflector. The reflector improves illumination on the higher wavelengths and reduces thermal load into the enclosure. After calibration the exact spectral range of the spectrograph was detected to be 421–1021 nm with a spectral resolution of 5 nm. A small process air flow is used to prevent condensation on the window.

The analysis is carried out with Matlab (The Mathworks) in a centralized desktop computer that is also capable of visualizing video feeds from all the web cameras for monitoring purposes. Since all channels are measured by the same imaging detector, the analysis is performed simultaneously in all channels with a single image grab and analysis sequence. However, the intensities of the measured spectra have to be roughly equal between the lines, so that high enough but not saturated spectra are obtained. This is ensured by individually adjusting the voltage of the halogen lamps. The variations of the color temperature caused by the different voltages as well as by the aging of the lamps are compensated for by the adaptive calibration as explained in Section 2.4. The measurement locations of the seven XRF-assayed slurry lines analyzed in this study are indicated in Fig. 4. The lines were selected to contain concentrates and tailings in both copper and zinc circuits to enable a comprehensive testing of the spectral analysis.

2.3. Data collection

The data for this study were collected during the normal operation of the Pyhäsalmi concentration plant in June–August 2008. The small sample cutters used to re-sample the Courier primary sample lines were susceptible to blockage especially for the tailing samples. For this reason, the sizes of valid data sets for different sample lines vary and the data contain gaps during which no measurements were available.

For each slurry line, the VNIR spectrum was initially measured at 5 second intervals. To match the about 30 second long collection of slurry sample for the XRF analysis, the 6 latest spectra were averaged after every other spectrum measurement. Thus the final spectrum samples represent 30 second averages of the slurry spectrum and have a sampling interval of 10 s. The XRF analyzer assays were collected during the normal operation of the analyzer, and the sampling intervals vary from 5 to 20 min. The most important slurry lines are assayed twice during the analyzer cycle, which shortens their average XRF sampling interval.

Table 1 summarizes the amount of collected data and the average contents of the slurry lines. Solids content of the copper middlings tailing flow is not given because the corresponding XRF measurement was not properly calibrated at the time. During the measurement period, the copper concentrate and copper tailing were assayed twice in one XRF cycle, which explains why more XRF data are available from these lines. On the other hand, the spectrum measurement flows in the middlings flotation tailings in both copper and zinc circuits were prone to blockages, and thus less middlings tailing data were obtained. The mineral contents in the table are calculated from the iron, copper and zinc XRF assays under the assumption that all copper is contained by chalcopyrite, all zinc by sphalerite and all left-over iron by pyrite. Even though these assumptions are not exactly fulfilled due to the presence of other minerals (especially pyrrhotite), the values should give reasonable approximates for the real proportions of the minerals.

2.4. Modeling

Data-based modeling was applied to the measured VNIR reflectance spectra and XRF values to find the connection between the spectra and the assay information. The modeling part in this study follows quite closely the same approach that was already reported by Haavisto et al., (2008).

The obtained data were preprocessed first by reducing the dimension of the spectral measurements from 960 to 20 wavelengths.
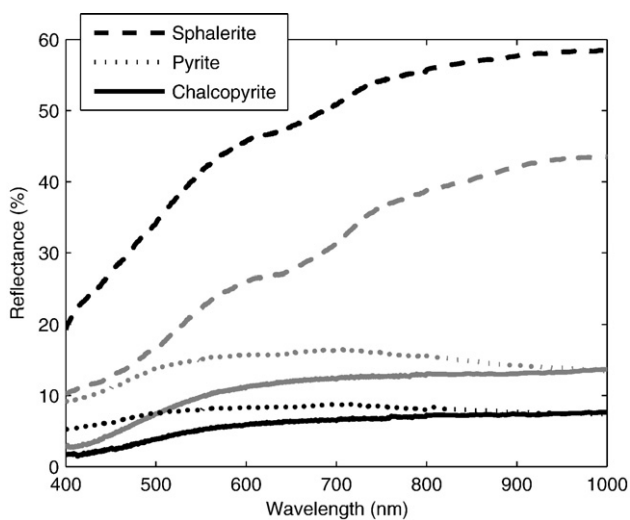

Fig. 1. Dry mineral reflectance spectra of the three main minerals contained by the analyzed ore. Particle sizes: 0–45 µm (black) and 45–125 µm (grey).
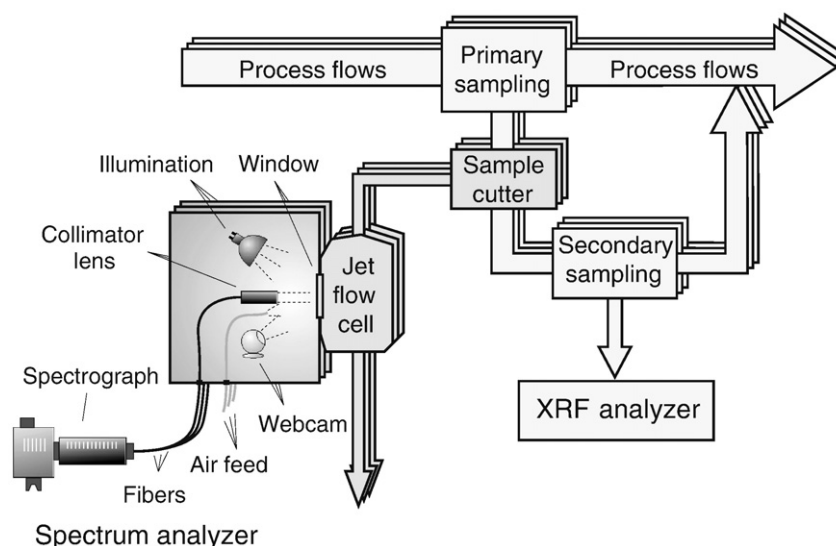
Fig. 2. The multichannel slurry spectrum analyzer cuts separate continuous slurry flows from the primary sample lines of the XRF analyzer. The spectrum analyzer was installed onto seven slurry lines, although only three are shown here.

The reflectances R were then transformed to absorbance values with the formula

$$A = \log(1 / R), \tag{1}$$

because according to the Beer–Lambert law, the absorbance A should be linearly proportional to the concentrations of the absorbing species in the target material (Ingle & Crouch, 1988). Even if the quite strict assumptions of the Beer–Lambert law are not completely fulfilled (as in this case due to the scattering caused by the small particle size, among others), the transformation is commonly used as a starting point in spectroscopic analysis (Osborne et al., 1993). Prior to the modeling, both the spectral data and XRF data were mean-centered.

The actual modeling was realized using the recursive partial least squares (rPLS) algorithm (Helland et al., 1991; Qin, 1993; Dayal & MacGregor, 1997b; Qin, 1998) based on the fast kernel PLS algorithm published by Dayal and MacGregor (1997a). The algorithm utilizes exponential forgetting (see e.g. Ljung and Söderström, 1983) to adaptively update the predictor x (VNIR spectrum) and response

y (XRF assay) autocovariance and cross-covariance matrix estimates on-line. Based on the covariance matrix estimates, a PLS model matrix B is calculated that can then be used to predict the assays from the spectra. The recursive adaptation of the model is done during the data collection. After acquiring the kth sample pair $\{x(k),y(k)\}$, the updated covariance matrix estimates $R_{xx}(k)$ and $R_{xy}(k)$ are calculated and further used by the kernel PLS algorithm to give the updated PLS coefficient matrix $B(k)$. The current PLS model $B(k)$ should now represent the best possible momentary calibration model between the spectra and the XRF assays, since the older data are exponentially forgotten (see Haavisto et al., 2008 for more details). Given a new spectrum x, the corresponding assay estimate $\hat{y}$ can be simply calculated by

$$\hat{y} = B(k)x. \tag{2}$$

3. Results and discussion

3.1. Measured spectra

The general properties of the different slurry line VNIR spectra were compared by calculating the average spectra for each line. Prior to averaging, the area under each individual spectrum was normalized to unity to compensate for the effect of the different illumination intensities between the lines. The averaged spectra are shown in Fig. 5(a). Both the spectrum of the illuminating light and the sensitivity of the used camera explain the weak intensities on the short and long wavelengths when compared with the middle region.

The effect of sphalerite and chalcopyrite on the spectrum is more clearly seen in the relative average reflectances calculated with respect to the average of the line averages (Fig. 5(b)). The spectra of the two concentrates differ the most from the overall average (i.e. one), whereas the tailing spectra are less distinctive. When compared to the content information given in Table 1, it is obvious that the high chalcopyrite and sphalerite percentages are the reason for the differences. In general, a higher sphalerite content tends to lead to higher relative reflectance values on the longer wavelengths and lower reflectances on the shorter wavelengths. Also, the average spectrum of the copper middlings tailing, where the sphalerite content is the highest of the tailings, seems to follow this rule.

Especially the effect of sphalerite in the measured VNIR spectra is well explained by the shape of the laboratory spectra of the powdered dry minerals (Fig. 1). According to the laboratory data, sphalerite is
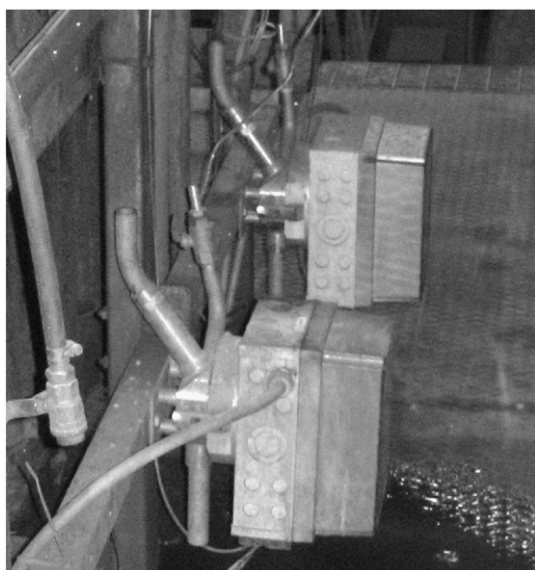

Fig. 3. Two spectrum analyzer boxes and jet flow cells installed at the concentration plant. The slurry tubes have not yet been connected.
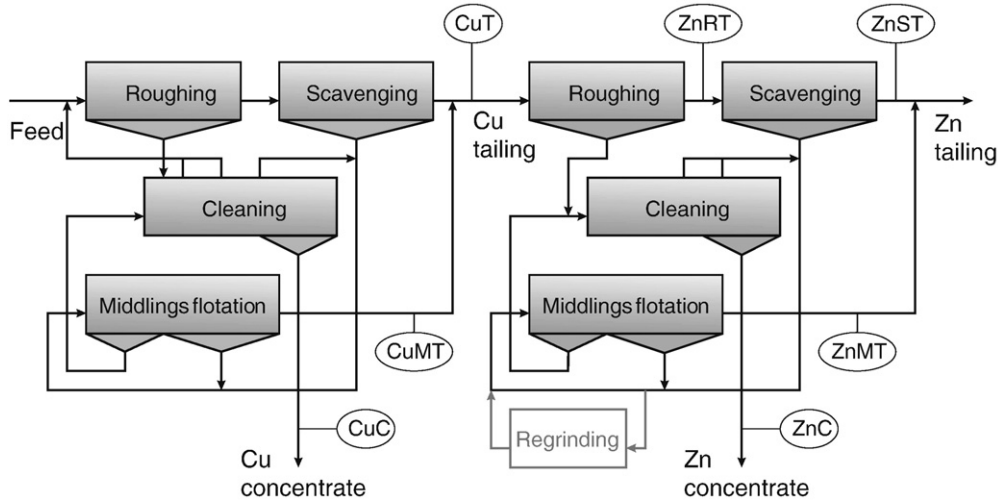
Fig. 4. The copper and zinc flotation circuits at Pyhäsalmi. The slurry lines analyzed in this study are: copper concentrate (CuC), copper middlings tailing (CuMT), copper tailing (CuT), zinc concentrate (ZnC), zinc rougher tailing (ZnRT), zinc scavenger tailing (ZnST), and zinc middlings tailing (ZnMT).

clearly distinguishable from the other two minerals due to its better overall reflectance. The longer wavelengths are also more emphasized in its spectrum, which corresponds to the acquired results. Curiously, smaller particle size seems to improve the reflectance of sphalerite, whereas the opposite is true for chalcopyrite and pyrite. The strong effect of the particle size on the slurry spectrum partially explains why an adaptive calibration algorithm is a necessity, since variations in the particle size distribution would easily invalidate a constant calibration model. On the other hand, with proper particle size reference data, the estimation of the particle size distribution based on spectra could also be possible.

3.2. Estimation results

The adaptive rPLS algorithm was applied separately to the data sets collected from each of the slurry lines. The optimal delay between the VNIR spectrum measurements and the XRF assays was computed from the data as in Haavisto et al. (2008), however this time the rPLS algorithm was used instead of the regular PLS. Seven latent variables were used in all PLS models, and a forgetting factor $\lambda = 0.95$ was utilized. The modeling performance was evaluated by comparing the PLS prediction

$$\hat{y}_{\mathrm{rpls}}(k) = B(k-1)x(k),\tag{3}$$

calculated using the previous PLS model $B(k-1)$ to the corresponding measured XRF assay $y(k)$. This validation scheme, as the normal cross-validation (see e.g. Ljung, 1999), has the important property that the data used in validation are not (yet) used for model estimation.

Additionally, since the validation is done right before the next model adaptation, the obtained results represent the model performance in the 'worst-case' situation. For each data set, the first 100 samples were reserved for model initialization and were not used for validation. Correspondingly, after a gap in the data longer than 1 h, the 10 following samples were not included in the validation to give the algorithm time to re-adapt.

The accuracy of the VNIR assay in all the lines is given in Table 2. For each line the coefficients of determination Q^2 (squared correlation coefficient for the validation data, see e.g. Toutenburg, 2002) are computed between the rPLS estimates (3) and the XRF assays. To describe the quality of the data, reference results for a 'dummy' zero-order hold (zoh) prediction (i.e. $\hat{y}_{\mathrm{zoh}}(k) = y(k-1)$) are also given in Table 2. The zoh values equal the squared autocovariances of the XRF assay time series with unit delay, thus describing how smoothly the assays change in time. Even though the PLS model is static and not dynamic, the rPLS method can be interpreted as a one-step predictor due to its adaptive nature: the previous XRF assay $y(k-1)$ is known by the model when the next value, $y(k)$, is estimated. Thus the rPLS coefficients of determination should be compared to the corresponding zoh values to better evaluate the accuracy of the VNIR assays.

The best assay estimates using the Q^2 criterion are obtained in the copper and zinc concentrates as well as in the copper middlings tailing. The zinc rougher tailing gives a fairly good iron estimate, however the more important zinc and copper values are rather poor. Also the performances of the other zinc tailing estimates excluding the solids content remain lower than the corresponding zoh values. In the two copper tailings the estimation is working better, especially

Table 1
The amount of data collected from the slurry lines, the average elemental and solids contents of the slurries measured by the XRF analyzer, and the calculated proportions of the main minerals.

Line	#XRF samples	#VNIR samples	Average elemental contents (%)				Average mineral contents (%)			Solids (%)
			Fe	Cu	Zn	S	Chalcopyrite	Sphalerite	Pyrite	
CuC	8598	885,983	29.70	29.66	2.60	35.23	85.66	4.06	7.56	28.34
CuMT	981	168,779	35.03	0.22	3.29	41.65	0.63	5.13	74.52	–
CuT	6848	719,183	35.83	0.05	2.14	42.07	0.14	3.34	76.67	33.76
ZnC	4303	857,723	9.34	0.87	52.35	33.49	2.51	81.72	13.37	32.23
ZnRT	3060	632,193	33.80	0.04	0.12	38.86	0.12	0.19	72.53	25.58
ZnST	4725	950,219	38.07	0.04	0.07	43.74	0.12	0.11	81.71	31.59
ZnMT	1939	373,858	36.57	0.08	0.17	42.06	0.23	0.27	78.40	16.95

C = concentrate, T = tailing, MT = middlings tailing, RT = rougher tailing, and ST = scavenger tailing.
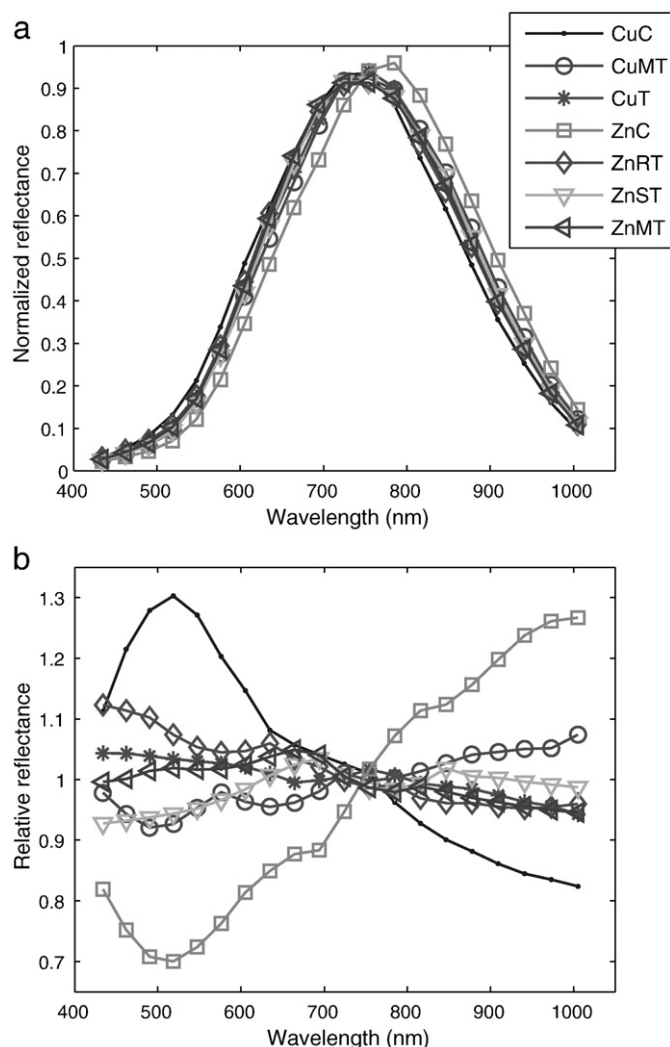
Fig. 5. (a) Average of the normalized spectra of the seven slurry lines and (b) the reflectance of the slurries relative to the overall average of the average spectra in (a).

Based on Table 2, it is obvious that the high chalcopyrite and sphalerite contents in the concentrates improve the accuracy of the VNIR spectral measurement. This is natural since these two minerals contain most of the copper and zinc detected by the XRF analyzer, and the higher the content values are, the more they affect the shape of the slurry spectrum captured by the spectrograph. Especially the zinc tailings with low sphalerite and chalcopyrite concentrates are more difficult to assay. The concentrates also favor the selected modeling approach, since there the grades are varying more regularly and the range of variation is rather large. In the tailings, on the other hand, the mineral contents typically remain quite low and constant for long periods of time, which degenerates the adaptive rPLS model and prevents the detection of sudden grade peaks. An alternative modeling method for these situations is presented and discussed by Haavisto and Hyötyniemi (2009). However, since the target of this study was to provide comparable results for all slurry lines, the highest disturbance peaks were omitted from the tailing data and the rPLS modeling method was applied to all lines.

3.3. High frequency assays

A high frequency slurry assay can be obtained from the VNIR spectra measured between the XRF assays. Assuming that the latest PLS model $B(k)$ calculated from the previous XRF assay $y(k)$ and the corresponding spectrum $x(k)$ is up-to-date, it can be used to estimate the assay information from all the spectra measured before the next XRF assay $y(k+1)$ is obtained. After that, the model can be updated.

Fig. 6 shows the high frequency assay of the copper content of copper concentrate and zinc content of zinc concentrate for a short period of time. Both the original VNIR assay and the low-pass filtered (90% exponential filtering) assay are shown. The copper measurement (Fig. 6(a)) clearly reveals that the copper content is heavily oscillating with a cycle time of about 10 min. Using only the XRF measurements even this slow oscillation could not be detected. The high frequency assay also provides a good starting point for diagnosing the cause of the oscillations, since, for example, spectrum analysis by Fourier transformation or autocovariance function calculation (Thornhill et al., 2003) can readily be performed.

the zinc content of the middlings tailing is estimated well, and even though the Q^2 for the copper estimate of the final copper tailing is as low as 0.5, it is clearly higher than the zoh value.

When determining the actual accuracy of the VNIR spectral measurement, it is important to note that also the XRF assays utilized in the rPLS calibration have a limited accuracy. According to the manufacturer (Anonymous, 2007), a relative standard deviation of 3–6% for minor concentrations and 1–4% for major concentrations should be achieved by the analyzer. A more comparable value of the XRF measurement accuracy is given by the calibration samples routinely collected at the concentration plant and analyzed in the laboratory. In Table 2, the coefficient of determination between the XRF assays and laboratory measurements for a set of calibration samples is given for each line. The calibration set sizes vary from 30 to 90 samples. Even though the calibration samples have been collected during an earlier period than the spectral measurements, they give a rough idea of the XRF analyzer's accuracy in the different slurry lines.

The XRF analyzer accuracy can restrict the obtained modeling performance between the detected VNIR spectra and the XRF assays. Generally, the XRF Q^2 values indicate that the XRF analyzer accuracy is on a good level, especially for zinc and copper, whereas the iron measurements are less accurate. An exceptionally low XRF Q^2 is given by the copper measurement in the zinc scavenger tailing, which explains the low accuracy of the corresponding rPLS estimate.

Table 2
Coefficients of determination (Q^2) between the rPLS estimated content values and the measured XRF assays.

Line	Result	Fe	Cu	Zn	SC
CuC	rPLS	**0.82**	**0.83**	**0.96**	**0.76**
	zoh	0.82	0.81	0.96	0.76
	XRF	0.72	0.93	0.98	0.77
CuMT	rPLS	**0.73**	0.77	**0.94**	–
	zoh	0.45	0.81	0.86	–
	XRF	0.41	0.93	0.96	0.95
CuT	rPLS	0.97	**0.50**	0.99	**0.67**
	zoh	0.98	0.34	1.00	0.37
	XRF	0.42	0.82	0.98	0.89
ZnC	rPLS	**0.87**	**0.95**	**0.89**	**0.90**
	zoh	0.80	0.98	0.84	0.73
	XRF	0.79	0.98	0.76	0.61
ZnRT	rPLS	**0.91**	0.57	0.78	**0.93**
	zoh	0.91	0.65	0.94	0.92
	XRF	0.80	0.79	0.97	0.72
ZnST	rPLS	0.95	0.17	0.64	**0.95**
	zoh	0.98	0.77	0.80	0.94
	XRF	0.66	0.04	0.98	0.83
ZnMT	rPLS	0.90	0.88	0.84	0.92
	zoh	0.93	0.93	0.91	0.93
	XRF	0.87	0.96	0.96	0.99

For a reference, the corresponding Q^2 values of a zero-order hold (zoh) predictor are also given. The XRF results are the Q^2 values between XRF assays and laboratory analysis for a different set of calibration samples. Bold numbers indicate the cases where rPLS gives an equally good or better Q^2 than zoh.
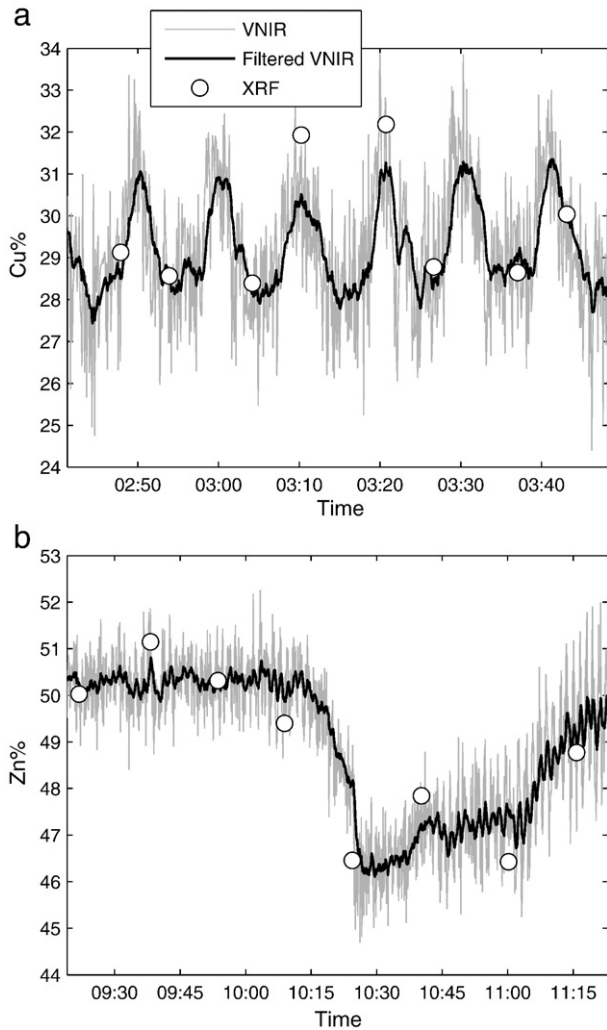
Fig. 6. The high frequency VNIR-based slurry assay indicating (a) rapid oscillations in the copper content of the copper concentrate and (b) a sudden drop in the zinc content of the zinc concentrate. 90% exponential filtering was used to calculate the low-pass filtered VNIR values. Also the corresponding sparse XRF assays are shown.

The zinc measurement (Fig. 6(b)), on the other hand, shows a large grade drop in the zinc concentrate indicating a disturbance in the zinc flotation circuit. Using the high frequency assays, this kind of major changes can be revealed sooner than with only the XRF analysis.

The high frequency assay of the zinc concentrate has been available for the process operators at the Pyhäsalmi concentration plant. The feedback has been positive: an operator interview revealed, for example, that since the improved assay gives a fast response to performed control actions, the operators can better evaluate the effect of the control changes they make.

4. Conclusions

This study has discussed the applicability of the VNIR reflectance spectrum assaying of slurry lines in copper and zinc flotation. The structure and installation of a fiber optic multichannel spectrum analyzer was described and the obtained spectra of the seven slurry lines were analyzed. It was shown that the average mineral contents clearly affect the general color of the slurry, and that especially the spectra of the zinc and copper concentrates can be distinguished easily due to their high sphalerite and chalcopyrite contents. A recursive PLS modeling algorithm was used to calculate and maintain on-line a valid linear calibration model between the spectra and the

XRF assays. The accuracy of the VNIR assay in all the lines was evaluated by comparing the coefficient of determination of the rPLS model with the dummy zero-order hold predictor. The VNIR assay was detected to give accurate assays especially for the concentrate lines with high sphalerite and chalcopyrite contents and regular grade variations. The assays of the copper middlings tailing flow were the best ones among the studied tailings.

The difficulty of VNIR-based assaying of the tailing flows is mainly due to the low sphalerite and chalcopyrite contents of the slurries. Also the blockage problems in these lines hindered the analysis, but a new sampling scheme is under development to solve this issue. Additionally, a more useful result would be the reliable and fast detection of sudden increases in the mineral grades of the tailings than an over-accurate analysis of the normally small content levels.

Finally, the high frequency VNIR assays were shown to provide new information especially on the concentrate grades, since the fast oscillations that are undetectable by the sparse XRF analysis can easily be revealed. Also the fast grade drops are shown earlier and more reliably by the VNIR analysis.

References

Anonymous, 2007. Courier® 6 SL — the high performance on-stream XRF slurry analyzer. Product brochure, available at http://www.outotec.com.

Bartolacci, G., Pelletier Jr., P., Tessier Jr., J., Duchesne, C., Bossé, P.-A., Fournier, J., 2006. Application of numerical image analysis to process diagnosis and physical parameter measurement in mineral processes—part I: flotation control based on froth textural characteristics. Miner. Eng. 19 (6–8), 734–747.

Clark, R.N., 1999. Spectroscopy of rocks and minerals, and principles of spectroscopy. In: Rencz, A.N. (Ed.), Manual of Remote Sensing, vol. 3. John Wiley and Sons, New York, pp. 3–58 (Ch. 1).

Dayal, B., MacGregor, J., 1997a. Improved PLS algorithms. J. Chemom. 7 (3), 169–179.

Dayal, B., MacGregor, J., 1997b. Recursive exponentially weighted PLS and its applications to adaptive control and prediction. J. Process Control 7 (3), 169–179.

Haavisto, O., Hyötyniemi, H., 2009. Recursive multimodel partial least squares estimation of mineral flotation slurry contents using optical reflectance spectra. Analytica Chimica Acta 642 (1–2), 102–109.

Haavisto, O., Kaartinen, J., Hyötyniemi, H., 2006. Optical spectrum based estimation of grades in mineral flotation. Proceedings of the IEEE International Conference on Industrial Technology. ICIT, Mumbai, India, pp. 2529–2534.

Haavisto, O., Kaartinen, J., Hyötyniemi, H., 2008. Optical spectrum based measurement of flotation slurry contents. Int. J. Miner. Process. 88 (3–4), 80–88.

Hapke, B., 1993. Theory of Reflectance and Emittance Spectroscopy. Topics in Remote Sensing. Cambridge University Press, Cambridge, UK.

Helland, K., Berntsen, H., Borgen, O., Martens, H., 1991. Recursive algorithm for partial least squares regression. Chemom. Intell. Lab. Syst. 14, 129–137.

Ingle, J.D., Crouch, S.R., 1988. Spectrochemical Analysis. Prentice-Hall, Englewood Cliffs, NJ.

Kaartinen, J., Hätönen, J., Hyötyniemi, H., Miettunen, J., 2006. Machine-vision-based control of zinc flotation — a case study. Contr. Eng. Pract. 14, 1455–1466.

Kruse, F.A., 1996. Identification and mapping of minerals in drill core using hyperspectral image analysis of infrared reflectance spectra. Int. J. Remote Sens. 17 (9), 1623–1632.

Liu, J., MacGregor, J., 2008. Froth-based modeling and control of flotation processes. Miner. Eng. 21 (9), 642–651.

Liu, J., MacGregor, J., Duchesne, C., Bartolacci, G., 2005. Flotation froth monitoring using multiresolutional multivariate image analysis. Miner. Eng. 18 (1), 65–76.

Ljung, L., 1999. System Identification, Theory for the User, 2nd Edition. Prentice Hall PTR, Upper Saddle River, NJ.

Ljung, L., Söderström, T., 1983. Theory and Practice of Recursive Identification. MIT Press, Cambridge, MIT.

McKee, D.J., 1991. Automatic flotation control — a review of 20 years of effort. Miner. Eng. 4 (7–11), 653–666.

Morar, S.H., Forbes, G., Heinrich, G.S., Bradshaw, D.J., King, D., Adair, B.J.I., Esdaile, L., 2005. The use of a colour parameter in a machine vision system, SmartFroth, to evaluate copper flotation performance at Rio Tinto's Kennecot copper concentrator. In: Jameson, G.J. (Ed.), Centenary of Flotation Symposium, Brisbane, Australia, 6–9 June 2005 — Proceedings. The Australasian Institute of Mining and Metallurgy, pp. 147–152. 6–9 June.

O. Haavisto, J. Kaartinen / Int. J. Miner. Process. 93 (2009) 187–193

193

Osborne, B.G., Fearn, T., Hindle, P.H., 1993. Practical NIR Spectroscopy with Applications in Food and Beverage Analysis. Longman, Harlow.

Qin, S., 1993. Partial least squares regression for recursive system identification. Proceedings of the 32nd Conference on Decision and Control, pp. 2617–2622. San Antonio, Texas.

Qin, S., 1998. Recursive PLS algorithms for adaptive data modeling. Comput. Chem. Eng. 22 (4/5), 503–514.

Thornhill, N., Huang, B., Zhang, H., 2003. Detection of multiple oscillations in control loops. J. Process Control 13 (1), 91–100.

Toutenburg, H., 2002. Statistical Analysis of Designed Experiments. Springer Texts in Statistics, 2nd Edition. Springer-Verlag, New York.